Bis(μ-silylene)-Bridged Dinuclear Rhodium(0) Complex and Its Palladium(0) and Platinum(0) Analogues. Theoretical Study of Their Electronic Structure, Bonding Nature, and Interconversion between μ-Disilene-Bridged Form and Bis(μ-silylene)-Bridged Form

Singo Nakajima, Daisuke Yokogawa, Yoshihide Nakao, Hirofumi Sato, and Shigeyoshi Sakaki*

Department of Molecular Engineering, Graduate School of Engineering, Kyoto University, Nishikyo-ku, Kyoto 615-8510

Received March 16, 2004

The dinuclear rhodium(0) complex with composition $Rh_2(Si_2H_4)(PH_3)_4$ is characterized as a bis(μ-silylene)-bridged dinuclear rhodium(0) complex with a Rh−Rh σ-bond, $Rh_2(\mu\text{-}SiH_2)_2(PH_3)_4$. In this complex, two d orbitals of one Rh center participate in the bonding interactions with the d_σ orbital of the other Rh center and the occupied sp^2 and unoccupied p orbitals of SiH_2. The palladium(0) analogue is characterized as a μ-disilene-bridged dinuclear complex with a Si═Si double bond and no Pd−Pd σ-bond, $Pd_2(\mu\text{-}Si_2H_4)(PH_3)_4$. On the other hand, the platinum(0) analogue is understood to be the bis(μ-silylene)-bridged dinuclear complex with a weak Si−Si bonding interaction, $Pt_2(\mu\text{-}SiH_2)_2(PH_3)_4$. It is theoretically proposed here that the interconversion between the bis(μ-silylene)-bridged form and the μ-disilene-bridged form is electrochemically achieved in the rhodium complex and that the palladium(0) and platinum(0) complexes, $Pd_2(\mu\text{-}Si_2H_4)(PH_3)_4$ and $Pt_2(\mu\text{-}SiH_2)_2(PH_3)_4$, are converted to the bis(μ-silylene)-bridged form with a M−M σ-bond (M = Pd or Pt), $[M_2(\mu\text{-}SiH_2)_2(PH_3)_4]^{2+}$, by two-electron oxidation with appropriate oxidant such as Cl_2, but the reverse, two-electron reduction, is electrochemically performed.

Introduction

Hydrosilane reacts with transition-metal complexes to afford a variety of compounds,[1] as shown by Scheme 1.[2−6] Some of them are considered models of intermediates and active species of transition-metal-catalyzed synthetic reactions of organic silicon compounds. Also, they are of considerable interest not only from the viewpoint of synthetic reaction but also from the viewpoint of electronic structure and bonding nature. For instance, there are two possible ways to understand dinuclear platinum(0) and palladium(0) complexes with composition $M_2(SiRR')_2(phoshine)_4$ (M = Pd or Pt; R, R′ = H, alkyl, aryl, etc.); one is a μ-disilene-bridged dinuclear complex with a Si═Si double bond, and the other is a bis(μ-silylene)-bridged dinuclear complex with four Pt−Si bonds and no Si−Si bond, as shown in Scheme 2. In a theoretical work with the extended Hückel MO method, it was reported that the short Si−Si distance of these complexes represented the presence of the Si−Si bonding interaction.[7] The P and S analogues were also theoretically investigated with the

Scheme 1

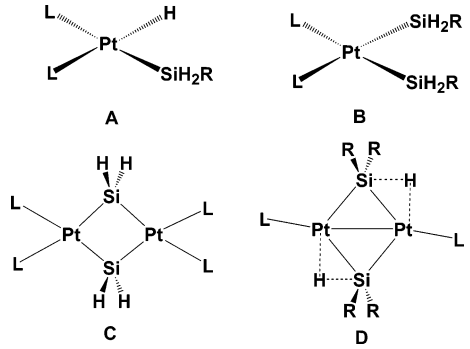

(1) (a) Schubert, U. *Angew. Chem., Int. Ed. Engl.* **1994**, *33*, 419. (b) Sharma, H. K.; Pannell, K. *Chem. Rev.* **1995**, *95*, 1351. (c) Ogino, H.; Tobita, H. *Adv. Organomet. Chem.* **1998**, *42*, 223. (d) Corey, J. Y.; Braddock-Wilking, J. *Chem. Rev.* **1999**, *99*, 175.

(2) (a) Zarate, Z. A.; Tessier-Youngs, C. A.; Youngs, W. J. *J. Am. Chem. Soc.* **1988**, *110*, 4068. (b) Zarate, Z. A.; Tessier-Youngs, C. A.; Youngs, W. J. *J. Chem. Soc., Chem. Commun.* **1989**, 577. (c) Sanow, L. M.; Chai, M.; McConnville, D. B.; Galat, K. J.; Simons, R. S.; Rinaldi, P. L.; Youngs, W. J.; Tessier, C. A. *Organometallics* **2000**, *19*, 192. (d) Simons, R. S.; Sanow, L. M.; Galat, K. J.; Tessier, C. A.; Youngs, W. J. *Organometallics* **2000**, *19*, 192.

(3) Michalczyk, M. J.; Recatto, C. A.; Calabrese, J. C.; Fink, M. F. *J. Am. Chem. Soc.* **1992**, *114*, 7955.

(4) Heyn R. H.; Tilley, T. D. *J. Am. Chem. Soc.* **1992**, *114*, 1917.

(5) (a) Kim, Y.-J.; Lee, S.-C.; Park, J.-I.; Osakada, K.; Choi, J.-C.; Yamamoto, T. *Organometallics* **1978**, *17*, 4929. (b) Kim, Y.-J.; Lee, S.-C.; Park, J.-I.; Osakada, K.; Choi, J.-C.; Yamamoto, T. *J. Chem. Soc., Dalton Trans.* **2000**, 417. (c) Osakada, K.; Tanaka, M.; Tanase, T. *Angew. Chem., Int. Ed.* **2000**, *39*, 4053. (d) Tanabe, M.; Yamada, T.; Osakada, K. *Organometallics* **2003**, *22*, 2190.

(6) (a) Levchinsky, Y.; Rath, N. P.; Braddock-Wiling, J. *Organometallics* **1999**, *18*, 2583. (b) Braddock-Wilking, J.; Levchinsky, Y.; Rath, N. H. *Organometallics* **2000,** *19*, 5500. (c) Braddock-Wilking, J.; Levchinsky, Y.; Rath, N. P. *Organometallics* **2001**, *20*, 474. (d) Braddock-Wilking, J.; Corey, J. Y.; Dill, K.; Rath, N. P. *Organometallics* **2002**, *21*, 5467.

10.1021/om040038a CCC: $27.50
Publication on Web 08/25/2004

Scheme 2

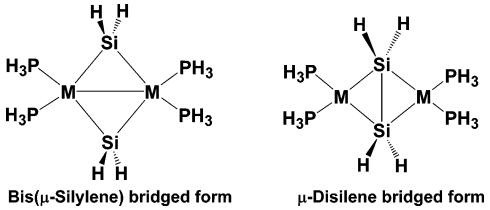

extended Hückel MO method.[8] However, the presence of the Si−Si bonding interaction is not universally accepted;[2c] actually, it is experimentally considered that the platinum(0) complex, $Pt_2(\mu\text{-}SiHR)_2(PR'_3)_4$ (R = hexyl; R′ = ethyl or propyl), consists of a four-membered Pt_2Si_2 ring.[2] Although a dotted line was drawn between two Si atoms to represent the Si−Si bonding interaction in a previous paper,[2c] the dotted line was omitted in a recent paper.[5d] In a theoretical study with the DFT method,[9] the platinum(0) complex was characterized as the bis(μ-silylene)-bridged dinuclear complex, but the palladium(0) analogue was understood to be the μ-disilene-bridged dinuclear complex. On the other hand, the disussion based on the extended Hückel MO calculations led to the prediction that the number of valence electrons determined whether the bis(μ-silylene)-bridged dinuclear form or the μ-disilene-bridged dinuclear one is the correct understanding of the dinuclear metal complex with composition $M_2(SiRR')(phosphine)_4$.[8] Thus, the correct characterization of this kind of dinuclear metal complexes is not simple and needs detailed computational analysis.

Besides the dinuclear palladium(0) and platinum(0) complexes, the similar bis(μ-silylene)-bridged dinuclear rhodium(0) complex, $Rh_2(\mu\text{-}SiRR')_2(dppe)_2$ (R = R′ = Ph, or R = Me, R′ = Ph; dppe = 1,2-bis(di-isopropylphosphino)ethane), was reported, recently.[10] The bonding interaction of this compound is schematically shown by four solid lines between Rh and Si atoms and a solid line between two Rh atoms;[10] in other words, this compound is understood to be a typical bis(μ-silylene)-bridged dinuclear complex with a Rh−Rh bond but no Si−Si bonding interaction. Thus, it is interesting to compare this rhodium(0) complex with the similar platinum(0) complexes such as $Pt_2(\mu\text{-}SiH_2)_2(dcpe)_2$ (dcpe = 1,2-bis(dicyclohexylphosphino)ethane),[3] $Pt_2(\mu\text{-}SiPh_2)_2(dmpe)_2$ (dmpe = 1,2-bis(dimethylphosphino)-ethane),[5a] and $Pt_2(\mu\text{-}SiR_2)_2(PMe_2Ph)_4$ (R = 2-isopropyl-6-methylphenyl).[6a] Also, it is an interesting research subject to synthesize the μ-disilene-bridged dinuclear rhodium complex and the bis(μ-silylene)-bridged dinuclear palladium complex by controlling d electron numbers. Despite the above-mentioned interesting issues of these complexes, no detailed theoretical study has been reported so far except for the recent theoretical study of the dinuclear palladium(0) and platinum(0) complexes.[9]

In this work, we theoretically investigated the rhodium(0), palladium(0), and platinum(0) complexes with composition $M_2(Si_2H_4)(PH_3)_4$ (M = Rh, Pd, or Pt). Our purposes here are to clarify the electronic structure and the bonding nature of these complexes, to make clear comparisons among these complexes, and to show how to achieve the interconversion between the bis(μ-silylene)-bridged form and the μ-disilene-bridged form in these complexes.

Computations

Geometries were optimized with the DFT method, where the B3LYP functional was used for exchange−correlation terms.[11,12] We ascertained that the optimized geometries did not exhibit any imaginary frequency. Energy and population changes were evaluated with the DFT, MP2 to MP4(SDQ), CCD, and CCSD(T) methods. In the CCSD(T) calculation, the contribution of triple excitations was incorporated noniteratively with single and double excitation wave functions.[13] Solvent effects were considered with the DPCM method[14] to evaluate the energy changes by two-electron reduction and two-electron oxidation reactions, because charged species are produced through these reactions.

Three kinds of basis set systems were mainly used. The smallest system (BS-I) was employed in the geometry optimization. In this BS-I system, core electrons of Rh (up to 3d), Pd (up to 3d), and Pt (up to 4f) were replaced with effective core potentials (ECPs), where a (341/321/21) set was used for valence electrons of Pt and (341/321/31) sets were employed for those of Rh and Pd.[15] For Si, P, and Cl, (21/21/1) sets were used,[16,17] where their core electrons (up to 2p) were replaced with ECPs. For H, the 6-31G set was employed.[18] The better basis set systems (BS-II and BS-III) were employed to evaluate energy and population changes. In the BS-II system, the same basis sets and ECPs as those of BS-I were used for Rh, Pd, Pt, P, and Cl. For Si and H, 6-311G(d) sets were employed.[19] In the BS-III system, a (541/541/111/1) set was used for the valence electrons of Pt and (541/541/211/1) sets were used for those of Rh and Pd with the same ECPs as those of the BS-I system.[20,21] A 6-311+G(d) set and a 6-311G(d) set[22] were used for Si and P, respectively, while the same basis set and ECPs as those of BS-I were used for Cl. In some calculations, a 6-31G(d) set[22] was employed for P to examine the basis set effects.

(7) Anderson, A. B.; Shiller, P.; Zarate, E. A.; Tessier-Youngs, C. A.; Youngs, W. J. *Organometallics* **1989**, *8*, 2320.
(8) (a) Alemany, P.; Alvarez, S. *Inorg. Chem.* **1991**, *31*, 4266. (b) Aullón, G.; Alemany, P.; Alvarez, S. *J. Organomet. Chem.* **1994**, *478*, 75.
(9) Sakaki, S.; Yamaguchi, S.; Musashi, Y.; Sugimoto, M. *J. Organomet. Chem.* **2001**, *635*, 173.
(10) (a) Fryzuk, M. D.; Rosenberg, L.; Rettig, S. J. *Organometallics* **1991**, *10*, 2537. (b) Fryzuk, M. D.; Rosenberg, L.; Rettig, S. J. *Organometallics* **1991**, *10*, 2871. (c) Fryzuk, M. D.; Rosenberg, L.; Rettig, S. J. *Inorg. Chim. Acta* **1974**, *222*, 345. (d) Rosenberg, L.; Fryzuk, M. D.; Rettig, S. J. *Organometallics* **1999**, *18*, 958.
(11) (a) Becke, A. D. *Phys. Rev. A* **1988**, *38*, 3098. (b) Becke, A. D. *J. Chem. Phys.* **1983**, *98*, 5648.
(12) Lee, C.; Yang, W.; Parr, R. G. *Phys. Rev. B* **1988**, *37*, 785.
(13) Cizek, J. *Adv. Chem. Phys.* **1969**, *14*, 35 (b) Purvis, G. D.; Bartlett, R. J. *J. Chem. Phys.* **1982**, *76*, 1910. (c) Scuseria, G. E.; Jansen, C. L.; Schaefer, H. F., III. *J. Chem. Phys.* **1988**, *89*, 7382. (d) Scuseria, G. E.; Schaefer, H. F., III. *J. Chem. Phys.* **1989**, *90*, 7382. (e) Pople, J. A.; Head-Gordon, M.; Raghavachari, K. *J. Chem. Phys.* **1987**, *87*, 5968.
(14) Miertus, S.; Scrocco, E.; Tomasi, J. *Chem. Phys.* **1981**, *55*, 117. Miertus, S.; Tomasi, J. *Chem. Phys.* **1982**, *65*, 239. Cossi, M.; Barone, V.; Cammi, R.; Tomasi, J. *Chem. Phys. Lett.* **1996**, *255*, 327.
(15) Hay, P. J.; Wadt, W. R. *J. Chem. Phys.* **1985**, *82*, 299.
(16) Wadt, W. R.; Hay, P. J. *J. Chem. Phys.* **1985**, *82*, 284.
(17) Höllwarth, A.; Böhme, M.; Dapprich, S.; Ehlers, A. W.; Gobbi, A.; Jonas, V.; Köhler, K. F.; Stegmann, R.; Veldkamp, A.; Frenking, G. *Chem. Phys. Lett.* **1993**, *208*, 237.
(18) Hehre, W. J.; Ditchfield, R.; Pople, J. A. *J. Chem. Phys.* **1972**, *56*, 2257.
(19) McLean, A. D.; Chandler, G. S. *J. Chem. Phys.* **1980**, *72*, 5639.
(20) Couty, M.; Hall, M. B. *J. Comput. Chem.* **1996**, *17*, 1359.
(21) Ehlers, A. W.; Böhme, M.; Dapprich, S.; Gobbi, A.; Höllwarth, A.; Jonas, V.; Köhler, K. F.; Stegmann, P.; Veldkamp, A.; Frenking, G. *Chem. Phys. Lett.* **1993**, *208*, 111.
(22) Francl, M. M.; Pietro, W. J.; Hehre, W. J.; Binkley, J. S.; Gordon, M. S.; DeFrees, D. J.; Pople, J. A. *J. Chem. Phys.* **1982**, *77*, 3654.

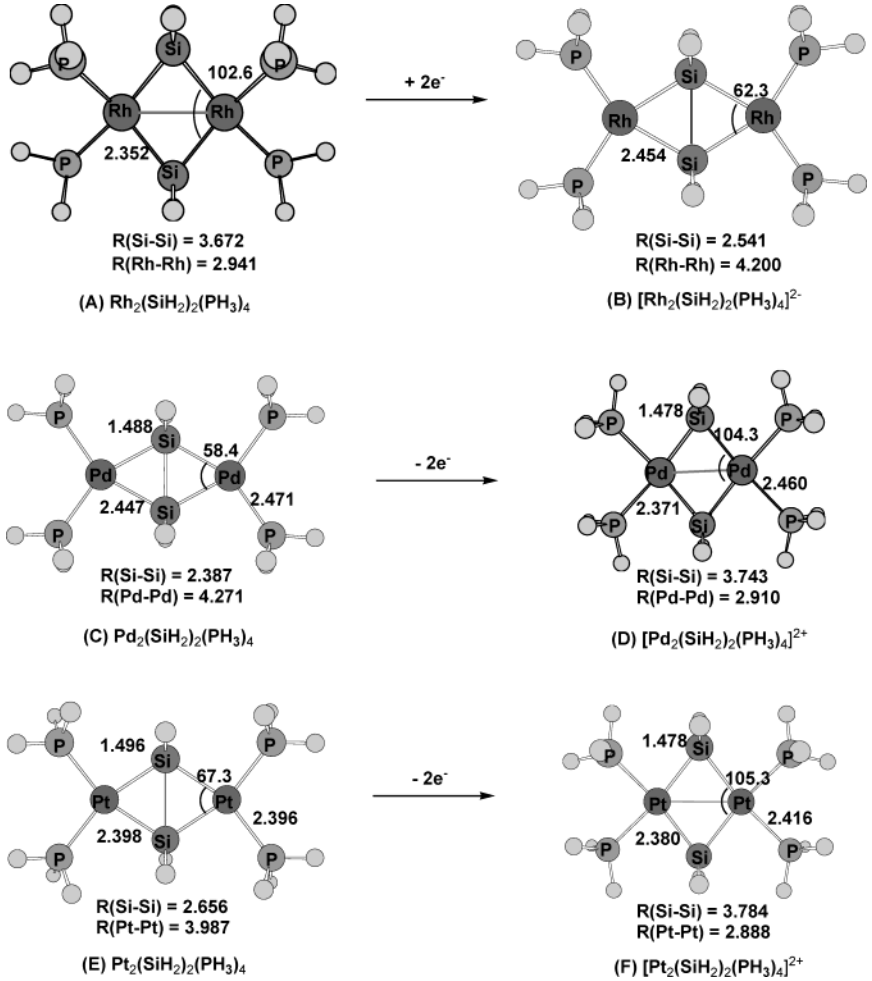

Figure 1. Optimzied geometries of rhodium, palladium, and platinum complexes with composition $M_2(SiH_2)_2(PH_3)_4$, $[M_2(SiH_2)_2(PH_3)_4]^{2-}$ (M = Rh), and $[M'_2(SiH_2)_2(PH_3)_4]^{2+}$ (M′ = Pd or Pt). Bond lengths in Å and bond angle in deg.

The Gaussian 98 program package was used for these calculations.[23] Population analysis was carried out with the method of Weinhold et al.[24] The contour map of molecular orbitals was drawn with the Molden program package.[25]

Results and Discussion

Bonding Nature and Electronic Structure of Bis(*μ*-silylene)-Bridged Dinuclear Rhodium(0) Complex, $Rh_2(\mu\text{-}SiH_2)_2(PH_3)_4$. The optimized geometry of $Rh_2(\mu\text{-}SiH_2)_2(PH_3)_4$ is shown in Figure 1 A, in comparison with those of the platinum(0) and palladium(0) analogues (Figure 1C,E). In the optimized geometry, two Rh, two Si, and four P atoms are on the same plane. This planar structure agrees with the experimental geometry in which two Rh and two Si atoms are on the same plane, but the positions of four P atoms slightly deviate from the plane.[10d,26] The optimized Rh−Rh distance (2.941 Å) agrees well with the experimental value (2.921 Å). Also, the Rh−Si distance (2.352 Å) agrees well with one of the experimental values (2.357 Å) but is considerably longer than the other experimental value (2.054 Å).[10d] Apparently, this Rh−Rh distance is much shorter than the Pd−Pd and Pt−Pt distances. Consistent with this short Rh−Rh distance, the Si−Si distance is much longer than those of the platinum(0) and palladium(0) analogues. These geometrical features suggest that a Rh−Rh bond is involved but a Si−Si bond is not in this complex.

In the rhodium(0) complex, the occupation number[24] of the Si−Si bond is zero and those of the Rh−Si bond are 1.674 e and 0.466 e for the *σ*- and *σ**-interactions, respectively, as shown in Table 1. These results show the presence of four Rh−Si bonds and the absence of the Si−Si bond, which are consistent with the geometrical features described above. However, the occupation number of the Rh−Rh bond is zero, which is not consistent with the experimental understanding that the Rh−Rh *σ*-bond is involved in the complex.[10] This issue will be discussed below in detail.

(23) Frisch, M. J.; Trucks, G. W.; Schlegel, H. B.; Scuseria, G. E.; Robb, M. A.; Cheeseman, J. R.; Zakrzewski, V. G.; Montgomery, J. A.; Stratmann, R. E.; Burant, J. C.; Dapprich, S.; Millam, J. M.; Daniels, A. D.; Kudin, K. N.; Strain, M. C.; Farkas, O.; Tomasi, J.; Barone, V.; Cossi, M.; Cammi, R.; Mennucci, B.; Pomelli, C.; Adamo, C.; Cliford, S.; Ochterski, J.; Petersson, G. A.; Ayala, P. Y.; Cui, Q.; Morokuma, K.; Malick, D. K.; Rabuck, A. D.; Raghavachari, K.; Foresman, J. B.; Cioslowski, J.; Ortiz, J. V.; Stefanov, B. B.; Liu, G.; Liashenko, A.; Piskorz, P.; Komaromi, I.; Gomperts, R.; Martin, R. L.; Fox, D. J.; Keith, T.; Al-Laham, M. A.; Peng, C. Y.; Nanayakkara, A.; Gonzalez, C.; Challacombe, M.; Gill, P. M. W.; Johnson, B. G.; Chen, W.; Wong, M. W.; Andres, J. L.; Head-Gordon, M.; Replogle, E. S.; Pople, J. A. *Gaussian 98*; Gaussian Inc.: Pittsburgh, PA, 1998.

(24) Reed, A. E.; Curtis, L. A.; Weinhold, F. *Chem. Rev.* **1988**, *88*, 849, and references therein.

(25) Schaftenaar, G.; Noordik, J. H. *J. Comput.-Aided Mol. Des.* **2000**, *14*, 123.

(26) The sum of bond angles around the Rh atom is 351.6°, and the sum of the interior angles of the Rh_2Si_2 four-membered ring is 359.95°.[10d]

Table 1. Occupation Numbers from NBO Analysis[a]

	Si−Si				M−Si	
	σ	σ^*	π	π^*	σ	σ^*
$Rh_2(\mu\text{-}SiH_2)_2(PH_3)_4$	0.0	0.0	0.0	0.0	1.674	0.466
$[Rh_2(\mu\text{-}SiH_2)_2(PH_3)_4]^{2-}$	1.775	0.323	1.531	0.619	0.0	0.0
$Pd_2(\mu\text{-}SiH_2)_2(PH_3)_4$	1.837	0.163	1.601	0.516	0.0	0.0
$[Pd_2(\mu\text{-}SiH_2)_2(PH_3)_4]^{2+}$	0.0	0.0	0.0	0.0	1.683	0.521
$Pt_2(\mu\text{-}SiH_2)_2(PH_3)_4$	1.756	0.209	0.0	0.0	0.0	0.0
	(1.727)[b]	(0.237)[b]	(0.0)[b]	(0.0)[b]	(0.0)[b]	(0.0)[b]
$[Pt_2(\mu\text{-}SiH_2)_2(PH_3)_4]^{2+}$	0.0	0.0	0.0	0.0	1.674	0.442

[a] The DFT/BS-III method was employed. [b] In parentheses are occupation numbers calculated by the CCD/BS-III method.

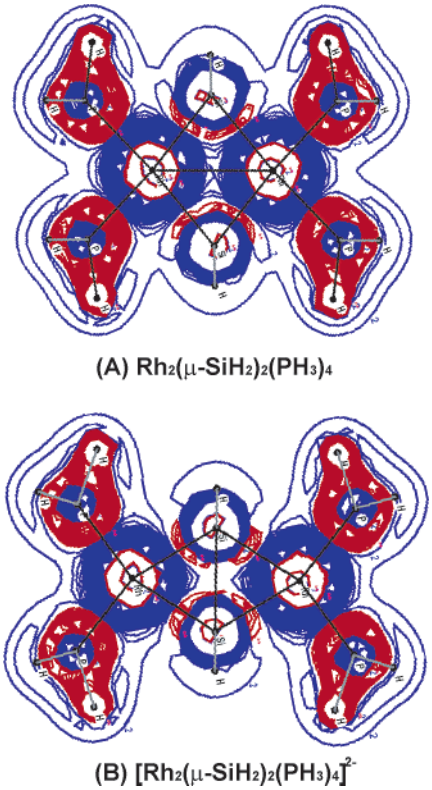

Figure 2. Laplacian of electron density of $Rh_2(\mu\text{-}SiH_2)_2(PH_3)_4$ and $[Rh_2(\mu\text{-}Si_2H_4)(PH_3)_4]^{2-}$. Contour values are 0.0, ±0.005, ±0.010, ±0.015, ... Blue and red lines represent positive and negative values, respectively.

We also investigated the Laplacian of electron density, where it is noted that electron accumulation occurs in the area where the Laplacian of electron density is negative.[24] The areas with the negative value are observed around two Si atoms, as shown in Figure 2A. This result is not consistent with the simple idea about the bonding interaction between Rh and SiH_2 groups, as follows: Because SiH_2 takes a singlet spin state in the ground state when substituents on the Si atom are not bulky,[27] the sp^2 lone pair orbital of SiH_2 is doubly occupied and one p orbital perpendicular to the SiH_2 plane is unoccupied, as shown in Scheme 3. This understanding suggests that the doubly occupied sp^2 orbital gives rise to the exchange repulsion with the doubly occupied $d_\sigma-d_\sigma$ bonding couple of the Rh−Rh moiety, but the unoccupied p orbital of SiH_2 forms a bonding interaction with the doubly occupied d_π orbital of Rh, as shown in Scheme 4A. This bonding picture leads us to the expectation that the Laplacian of electron density should be negative in the area where the unoccupied p orbital of SiH_2 overlaps with the d_π orbital of Rh, but it should be positive in the area where the sp^2 orbital of SiH_2 overlaps with the d_σ-d_σ bonding orbital of the Rh−Rh moiety. Apparently, this expectation does not agree with Figure 2A.

Scheme 3

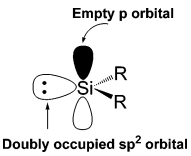

Scheme 4[a]

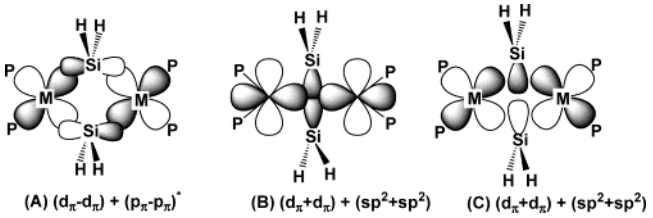

[a] The p_π and sp^2 orbitals belong to SiH_2. The signs + and − represent bonding and antibonding interaction, respectively.

To understand the bonding interactions and Laplacian of electron density, we will inspect here the molecular orbitals of this compound. In Figure 3, several important Kohn−Sham orbitals are shown, where Hartree−Fock orbitals are omitted for brevity because they are similar to Kohn−Sham orbitals (see Supporting Information Figures S-1 and S-2 for Hartree−Fock orbitals and the other Kohn−Sham orbitals near the HOMO and LUMO). Important results are summarized, as follows: (1) The HOMO-10 orbital includes the bonding overlap between the d_σ orbital of Rh and the d_σ orbital of the other Rh, and the LUMO includes its antibonding counterpart, where the "HOMO-*m*" represents the *m*th orbital from the HOMO in the occupied space. (2) The HOMO-10 orbital also involves the bonding interaction between the sp^2 orbital of SiH_2 and the $d_\sigma-d_\sigma$ bonding couple of the Rh−Rh moiety. This orbital corresponds to the interaction shown by Scheme 4B. (3) However, its antibonding counterpart is not involved in the occupied space. If the antibonding counterpart was involved in the occupied space, the sp^2 orbital would totally give rise to the exchange repulsion with the doubly occupied $d_\sigma-d_\sigma$ bonding couple, as expected above. The absence of the antibonding counterpart in the occupied space indicates that the $d_\sigma-d_\sigma$ bonding couple of the Rh−Rh moiety forms a bonding interaction with the sp^2 orbitals of two SiH_2 groups. (4) The unoccupied p orbital of SiH_2 overlaps well with the d_π orbital of Rh in a bonding way to form the HOMO-5

(27) Gordon, M. S. *Chem. Phys. Lett.* **1985**, *114*, 348.

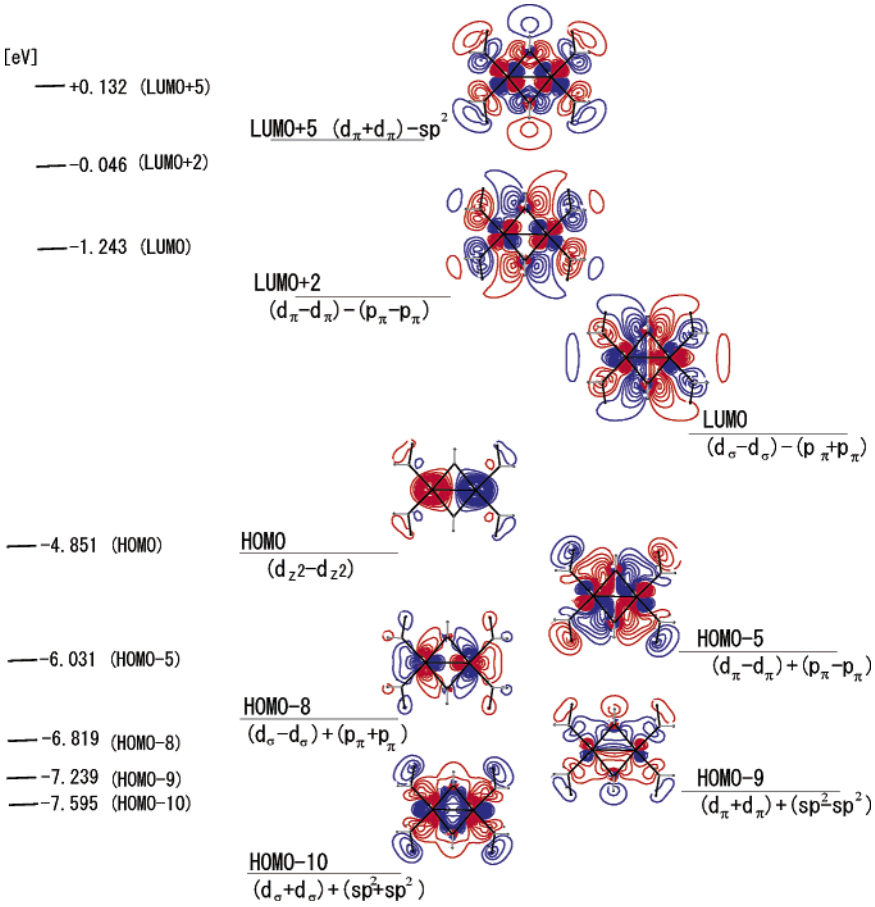

Figure 3. Kohn−Sham orbitals of $Rh_2(\mu\text{-}SiH_2)_2(PH_3)_4$. Values are Kohn−Sham orbital energies (in eV). Contour values are 0.0, ±0.025, ±0.050, ±0.075, ... Blue and red lines represent positive and negative values, respectively.

orbital, which corresponds to the π-back-donation interaction, as shown in Scheme 4A. Its antibonding counterpart is observed in the LUMO+2 orbital, where "LUMO+*n*" represents the *n*th orbital from the LUMO in the unoccupied space. These features indicate that the π-back-donation from the d_π orbital of Rh to the unoccupied p orbital of SiH_2 plays an important role in the bonding interaction. (5) In the HOMO-9 orbital, the sp^2 orbital of SiH_2 overlaps with the sp^2 orbital of the other SiH_2 group in an antibonding way, because the sp^2 orbital of SiH_2 is doubly occupied. This HOMO-9 orbital also involves the bonding overlap between the d_π orbital of Rh and the sp^2 orbital of SiH_2, as shown in Scheme 4C. (6) The LUMO+5 orbital involves the antibonding overlap between the sp^2 orbital of SiH_2 and the $d_\pi-d_\pi$ bonding couple of the Rh−Rh moiety, while the HOMO-8 orbital involves the bonding overlap between the unoccupied p orbital of SiH_2 and the $d_\sigma-d_\sigma$ antibonding couple of the Rh−Rh moiety. These features of HOMO-8 and LUMO+5 orbitals are against our expectation on the basis of simple understanding, as follows: In the simple understanding, this compound is considered to consist of the d^9-d^9 system and two SiH_2 moieties, in which only the $d_\sigma-d_\sigma$ antibonding orbital is unoccupied but both the $d_\pi-d_\pi$ bonding orbital of the Rh−Rh moiety and the sp^2 orbital of SiH_2 are doubly occupied except for the antibonding counterpart of the π-back-donation orbital, which consists of the $d_\pi-d_\pi$ antibonding couple of the Rh−Rh moiety and the unoccupied p orbital of SiH_2. This simple understanding leads to the picture that the LUMO+5 orbital should be doubly occupied because this orbital mainly consists of two d_π orbitals of Rh and two sp^2 orbitals of SiH_2 but the HOMO-8 orbital should be unoccupied groups because this orbital consists of the $d_\sigma-d_\sigma$ antibonding couple and the p orbital of SiH_2. We carried out the DFT calculation in which the HOMO-8 orbital is exchanged with the LUMO+5 orbital. However, the converged electronic structure is the same as that before the exchange. From these results, it is concluded that the electronic structure of this complex differs from the simple understanding mentioned above.

The above discussion provides us with the correct understanding of the bonding nature of $Rh_2(\mu\text{-}SiH_2)_2(PH_3)_4$. In a typical rhodium(I) complex with a d^8 electron configuration, one d orbital is basically unoccupied and it participates in the bonding interaction with ligands. In a typical dinuclear rhodium(0) complex with a Rh−Rh σ-bond, one $d_\sigma-d_\sigma$ bonding couple is doubly occupied and its antibonding counterpart is unoccupied. Here, we will investigate such an ideal dinuclear rhodium(0) complex as $Rh_2(SiH_2)_2(PH_3)_4$, which involves the Rh−Rh σ-bond without a bridging ligand. The optimized geometry of this complex is shown in Figure 4, where the Rh−Rh−Si angle was fixed at 90°; if not, the geometry optimization led to the bis(μ-silylene)-bridged structure.[28] Obviously, the Rh−Rh distance is very short (2.565 Å), which clearly shows the presence of the typical Rh−Rh σ-bond. Consistent with

(28) This geometry is calculated to be much less stable than $Rh_2(\mu\text{-}SiH_2)_2(PH_3)_4$ by 75.5, 59.5, 65.5, 53.9, and 45.1 kcal/mol with DFT, MP2, MP3, MP4(DQ), and MP4(SDQ)/BS-II methods, respectively.

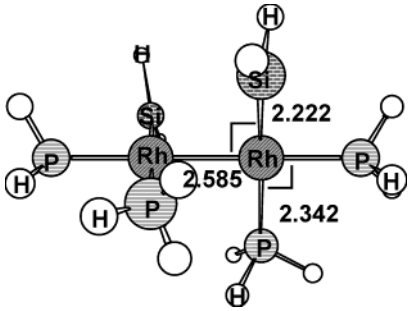

Figure 4. Optimized geometries of $Rh_2(SiH_2)_2(PH_3)_4$ possessing nonbridged SiH_2. PRhP and SiRhRh angles are assumed to be 90°.

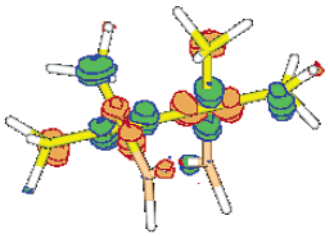

LUMO+2 (-0.749 eV)

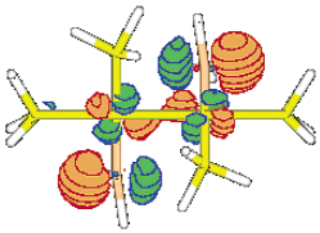

LUMO (-1.981 eV)

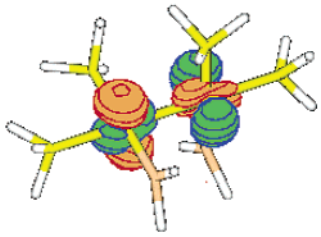

HOMO (-4.834 eV)

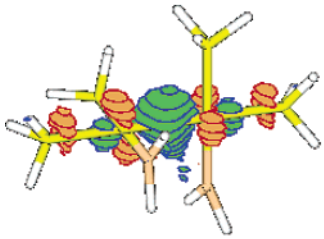

HOMO-4 (-5.288 eV)

Figure 5. Important Kohn−Sham orbitals of $Rh_2(SiH_2)_2(PH_3)_4$ possessing nonbridging SiH_2. Contour values are 0.0, ±0.025, ±0.050, ±0.075, ... Blue and red lines represent positive and negative values, respectively.

this short Rh−Rh distance, the $d_\sigma-d_\sigma$ bonding overlap is involved in the HOMO-4 orbital and its antibonding counterpart is in the LUMO+2 orbital, as shown in Figure 5. This feature indicates that one d_σ orbital of Rh forms one $d_\sigma-d_\sigma$ bonding interaction with the d_σ orbital of the other Rh in $Rh_2(SiH_2)_2(PH_3)_4$. In $Rh_2(\mu\text{-}SiH_2)_2(PH_3)_4$, one d_σ orbital of Rh forms one bonding interaction with the d_σ orbital of the other Rh like the Rh−Rh σ-bond of $Rh_2(SiH_2)_2(PH_3)_4$, as shown by the presence of the HOMO-10 orbital and the LUMO. In addition to this $d_\sigma-d_\sigma$ bonding orbital, one $d_\pi-d_\pi$ bonding couple forms a bonding interaction with the unoccupied p orbital of SiH_2, expectedly, and with the doubly occupied sp^2 orbital of two SiH_2 groups, unexpectedly, as shown by the presence of HOMO-5, HOMO-8, and LUMO+5 orbitals. Thus, it is concluded that two d orbitals of Rh participate in the bonding interactions, although the Rh atom takes a d^9 electron configuration in a formal sense.

Let's return to the Laplacian of electron density. As discussed above, the SiH_2 moiety forms three types of bonding interactions, as shown in Scheme 4A−C. This means that electron accumulation occurs in the areas where the unoccupied p and occupied sp^2 orbitals of SiH_2 overlap with the d_π and d_σ orbitals of Rh, respectively. As a result, the Laplacian of electron density becomes negative in the area surrounding the Si atom, as shown in Figure 2A. Although the Rh−Rh σ-bond is formed, as discussed above, the Rh−Rh σ-bond is not displayed by the NBO analysis and the Laplacian of electron density. This is interpreted in terms of the presence of the HOMO-8 orbital; because this orbital involves a $d_\sigma-d_\sigma$ antibonding overlap into which the p orbital of the SiH_2 group mixes in a bonding way, the Rh−Rh bonding interaction becomes weak and the Rh−SiH_2 bonding interaction becomes strong. Thus, the Rh−Rh bond is not displayed, but the Rh−SiH_2 bond is displayed by the NBO analysis and the Laplacian of electron density.

Two-Electron Reduction of Bis(*μ*-silylene)-Bridged Dinuclear Rhodium(0) Complex. Two-electron reduction of the bis(μ-silylene)-bridged dinuclear rhodium(0) complex induces significantly large geometry changes, as shown in Figure 1B. Apparently, the Si−Si distance considerably shortens and the Rh−Rh distance substantially lengthens. Consistent with these geometry changes, the occupation number of the Rh−Si bond becomes zero, and the π and π^* orbitals of the Si═Si double bond exhibit a substantially large occupancy number and a moderately large one, respectively. The Laplacian of electron density is negative in the areas around Si atoms, and these areas contact with each other, as shown in Figure 2B. These features indicate the presence of the Si−Si bonding interaction. Thus, it should be concluded that the bis(μ-silylene)-bridged dinuclear rhodium(0) complex is converted to the μ-disilene-bridged dinuclear rhodium complex, $[Rh_2(\mu\text{-}Si_2H_4)(PH_3)_4]^{2-}$, by two-electron reduction.

The electronic structure and the bonding nature of this complex are easily interpreted in terms of the orbital correlation diagram of Figure 6, as follows: The LUMO of $Rh_2(\mu\text{-}SiH_2)_2(PH_3)_4$ becomes doubly occupied by two-electron reduction. Because the LUMO mainly consists of the $d_\sigma-d_\sigma$ antibonding overlap, the Rh−Rh σ-bond is broken by the two-electron reduction, which increases the Rh−Rh distance. This allows mutual approach of two SiH_2 groups to each other, to form the Si−Si bonding interaction. Certainly, the π-bond of disilene is formed in the HOMO of $[Rh_2(\mu\text{-}Si_2H_2)(PH_3)_4]^{2-}$, as shown in Figure 6. At the same time, the HOMO-5 orbital of $Rh_2(\mu\text{-}SiH_2)_2(PH_3)_4$ changes into the HOMO-9 orbital in $[Rh_2(\mu\text{-}Si_2H_4)(PH_3)_4]^{2-}$, where the HOMO-9 orbital involves the π-back-donation from the

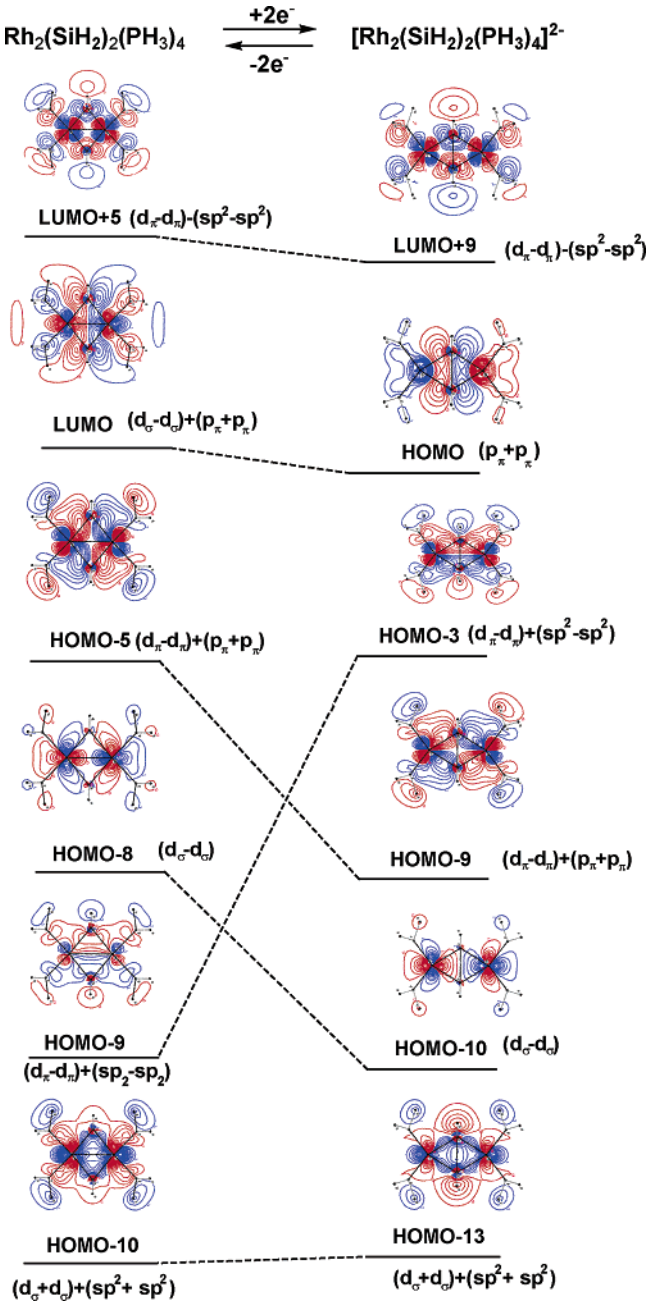

Figure 6. Correlation diagram of several important Kohn−Sham orbitals upon two-electron reduction of $Rh_2(\mu\text{-}SiH_2)_2(PH_3)_4$. Contour values are 0.0, ±0.025, ±0.050, ±0.075, ... Blue and red lines represent positive and negative values, respectively.

d_π orbital of Rh to the π^* orbital of disilene. Seemingly, the mutual approach of two Si atoms enhances the σ-type antibonding overlap between two sp^2 orbitals of SiH_2 in the HOMO-9 orbital of $Rh_2(\mu\text{-}SiH_2)_2(PH_3)_4$. However, this HOMO-9 orbital changes into the HOMO-3 orbital of $[Rh_2(\mu\text{-}Si_2H_4)(PH_3)_4]^{2-}$, in which the d_π component becomes predominant. On the other hand, the σ^*-antibonding overlap between two sp^2 orbitals becomes predominant in the LUMO+5 orbital. These orbital changes correspond to the polarization which decreases the antibonding interaction between the two SiH_2 groups and increases the d_π component in the occupied space. As a result, all d orbitals are doubly occupied in $[Rh_2(\mu\text{-}Si_2H_4)(PH_3)_4]^{2-}$ and the Si═Si double bond is formed. The resultant electronic structure is the same as that of the dinuclear palladium(0) complex, as will be discussed below.

As shown in Table 2, the reaction energy by the two-electron reduction considerably fluctuates upon going from MP2 to MP4(DQ) and moderately fluctuates upon going to CCSD(T) from MP4(DQ) in BS-II. This fluctuation cannot be improved by using the triple-ζ basis set for P and better basis sets for Si and Rh (see Supporting Information, Table S-2). The reaction energies by DFT and MP4(SDQ) become similar to each other upon improving the basis sets, while the difference in the energy between the CCSD(T) and MP4(SDQ) methods is not small even in the better basis sets here.[29a] Thus, the best value for the reaction energy is still ambiguous at the present time.[29b] However, the reaction energy is moderate in all the calculations, compared with those of the two-electron oxidation of the platinum(0) and palladium(0) complexes, which will be discussed below. These results suggest that the two-electron reduction of $Rh_2(\mu\text{-}SiH_2)_2(PH_3)_4$ is easily achieved electrochemically. This reaction energy is significantly influenced by incorporation of solvent effects; the DPCM method indicates that the two-electron reduction becomes exothermic in THF,[30] as shown in Table 2. This suggests that the relative stabilities of these two forms are controlled by selecting an appropriate solvent.

Changes of electron population induced by two-electron reduction are shown in Table 3. The Rh atomic population moderately increases by 0.108 e, and the electron population of PH_3 somewhat increases by 0.276 e. In the Rh atom, the d orbital population increases by 0.036 e and the s orbital population increases by 0.059 e. On the other hand, the sum of electron populations of the two SiH_2 moieties considerably increases by 0.681e. In other words, the two electrons added to the molecule are not localized in the d orbital of Rh but delocalized over the whole molecule, in particular, on the Si_2H_4 moiety. These results indicate that the π-back-donation from the d_π orbital of Rh to the π^* orbital of Si_2H_4 is much stronger in $[Rh_2(\mu\text{-}Si_2H_4)(PH_3)_4]^{2-}$ than that from the d_π orbital of Rh to the p orbital of SiH_2 in $Rh_2(\mu\text{-}SiH_2)_2(PH_3)_4$, as expected.

Electronic Structure and Bonding Nature of Platinum(0) and Palladium(0) Analogues. As shown in Figure 6, the $d_\sigma-d_\sigma$ antibonding orbital is doubly occupied in these complexes like $[Rh_2(\mu\text{-}SiH_2)_2(PH_3)_4]^{2-}$. This clearly shows that the M−M σ-bond is not involved

(29) (a) Here, the reaction energy seems to converge upon going to MP4(SDQ) from MP2, except for the MP3 method. Further, the MP4(SDQ) method provides a reaction energy similar to that of the DFT method. Also, the energy by the MP3 method deviates in general from those by the MP2 and MP4 methods. Thus, the present results are not very bad. One problem is that the reaction energy by the CCSD(T) method decreases upon improving the basis set, but it is still considerably different from those of the DFT and MP4(SDQ) methods (see Supporting Information, Table S-2). (b) The CAS-SCF/PT2 method would provide reliable results of the present systems. However, the complexes investigated are too large to be calculated with the CAS-SCF/PT2 method, because 10 d orbitals of two Rh atoms and two p and two sp^2 orbitals of two SiH_2 groups should be involved in the active space of the CAS-SCF calculation. Although these systems should be investigated with a better method, we believe that the present results provide a semiquantitatively correct discussion, at least.

(30) The solvation energy was calculated with the geometries optimized in the gas phase, where the nonelectrostatic terms were included. THF was employed here as one of the typical solvents. Its parameters implemented in the Gaussian 98 program were used without any modification for the DPCM calculation; for instance, permittivity is 7.58.

Table 2. Energy Changes (in kcal/mol) between $Rh_2(\mu\text{-}SiH_2)_2(PH_3)_4$ and $[Rh_2(\mu\text{-}SiH_2)_2(PH_3)_4]^{2-}$ and between $M_2(\mu\text{-}SiH_2)_2(PH_3)_4$ and $[M_2(\mu\text{-}SiH_2)_2(PH_3)_4]^{2+}$ (M = Pd or Pt)

(A) $M_2(\mu\text{-}Si_2H_4)(PH_3)_4 \rightarrow [M_2(\mu\text{-}Si_2H_4)(PH_3)_4]^{2-\text{ or }2+}$

	$Rh_2(\mu\text{-}SiH_2)_2(PH_3)_4$ two-electron reduction		$Pd_2(\mu\text{-}Si_2H_4)(PH_3)_4$ two-electron oxidation		$Pt_2(\mu\text{-}Si_2H_4)(PH_3)_4$ two-electron oxidation	
	BS-II	BS-III	BS-II	BS-III	BS-II	BS-III
DFT	36.0	30.4 (−108.2)[a]	346.4	346.0 (215.7)[a]	350.3	340.0 (207.8)[a]
MP2	61.5	48.8	319.6	320.3	322.5	313.0
MP3	78.8	76.1	321.2	321.6	325.3	314.9
MP4(DQ)	59.7	46.3	322.4	324.9	326.1	317.0
MP4(SDQ)	50.5	35.8	324.1	326.9	327.1	318.8
CCSD	68.2		322.3		326.2	
CCSD(T)	64.0		322.3		326.4	

(B) $M_2(\mu\text{-}Si_2H_4)(PH_3)_4 + Cl_2 \rightarrow [M_2(\mu\text{-}Si_2H_4)(PH_3)_4]Cl_2$

	M = Pd		M = Pt	
	BS-II	BS-III	BS-II	BS-III
DFT	−16.7	−20.2 (−45.3)[a]	−6.6	−17.6 (−39.1)[a]
MP2	−43.9	−47.8	−33.3	−47.4
MP3	−32.0	−36.6	−18.6	−33.2
MP4(DQ)	−31.9	−36.1	−21.5	−35.4
MP4(SDQ)	−32.2	−36.3	−22.0	−35.5

[a] The solvent effects of THF were taken into consideration with the DPCM method.

Table 3. Population Changes[a] by Two-Electron Reduction of $Rh_2(\mu\text{-}SiH_2)_2(PH_3)_4$ and Two-Electron Oxidation of $M_2(\mu\text{-}SiH_2)_2(PH_3)_4$ (M = Pd or Pt)

	$[Rh_2(SiH_2)_2(PH_3)_4]^n$		$[Pd_2(SiH_2)_2(PH_3)_4]^n$		$[Pt_2(SiH_2)_2(PH_3)_4]^n$	
	$n = 0$	$n = 2-$	$n = 0$	$n = 2+$	$n = 0$	$n = 2+$
M	45.615	45.723	46.084	46.003	78.224	78.130
s	2.451	2.493	2.481	2.488	2.712	2.720
p	6.004	6.012	6.009	6.014	6.015	6.021
d	9.159	9.218	9.594	9.500	9.497	9.387
Si_2H_4	31.790	32.471	32.277	31.561	32.187	31.550
PH_3[b]	17.745	18.021	17.889	17.607	17.841	17.548

[a] NBO population analysis. The DFT/BS-III method was employed. [b] Average value.

in these complexes, which is one of the characteristic differences between the rhodium(0) complex and these platinum(0) and palladium(0) analogues. As shown in Table 1, the occupation number of the Pd−Si bond is zero and those of the Si−Si bond are 1.837 e, 0.163 e, 1.601 e, and 0.516 e for the σ-, σ*-, π-, and π*-interactions, respectively. These results indicate that the palladium(0) complex is characterized as the μ-disilene-bridged complex $Pd_2(\mu\text{-}Si_2H_4)(PH_3)_4$, as previously reported.[9] In the platinum(0) analogue, the occupation numbers significantly depend on the basis sets used; the occupation number of the Si−Si bond is zero and that of the Pt−Si bond is 1.758 e and 0.197 e for the σ- and σ*-interactions, respectively, in the BS-II system, while the occupation number of the Pt−Si bond is zero but they are 1.756 e and 0.209 e for the σ- and σ*-interactions of the Si−Si bond, respectively, in the BS-III system. Almost the same occupation numbers are calculated with the CCD method, too, as shown in Table 1. Because the occupation number is zero for the π- and π*-interactions of the Si═Si bond in all the calculations, the platinum(0) complex cannot be characterized as a μ-disilene-bridged dinuclear complex. From these results, it is likely to conclude that the platinum(0) complex is characterized as rather a bis(μ-silylene)-bridged dinuclear complex with a weak Si−Si bonding interaction, $Pt_2(\mu\text{-}SiH_2)_2(PH_3)_4$, as shown in Scheme 5. Thus, it is not unreasonable that the previous theoretical study with the extended Hückel MO method proposed the presence of the Si−Si bonding interaction.[7]

Scheme 5

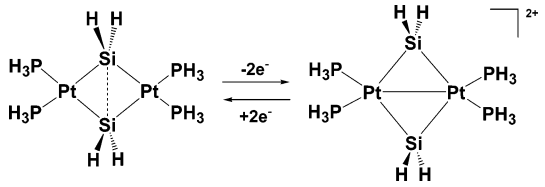

This difference between the palladium(0) and platinum(0) complexes was interpreted in terms of the energy level and the size of the d orbital. Because the d orbital of the Pt(0) atom is at a higher energy and more expanded toward Si_2H_4 than that of the Pd(0) atom,[31,32] the π-back-donation from the d_π orbital to the π* orbital of disilene is stronger in the platinum(0) complex than in the palladium(0) analogue, which weakens the Si−Si bond in the platinum(0) complex to a greater extent than in the palladium(0) complex (see Supporting Information, Figure S-3A). Also, the d_π−d_π bonding overlap is larger in the platinum(0) complex than that in the palladium(0) complex due to the larger expansion of the d orbital of Pt than that of Pd.[32] This leads to the

(31) (a) The 4d orbital energies of the Rh(0), Pd(0), and Pd(I) atoms are −16.6, −18.0, and −21.0 eV, respectively, and the 5d orbital energies of the Pt(0) and Pt(I) atoms are −16.9 and −20.4 eV, where these values were evaluated with the relativisitic Hartree−Fock method.[31b] (b) Fraga, S.; Saxena, K. M. S.; Karwowski, J. *Physical Science Data 5 Handbook of Atomic Data*; Elsevier: Amsterdam, 1976.

(32) The radius of maximum charge density of the valence d orbital is 0.60 Å for the Rh(0) atom, 0.55 Å for the Pd(0) atom, and 0.65 Å for the Pt(0) atom.[31b]

larger antibonding overlap between the two Si atoms in the platinum(0) complex than that in the palladium(0) complex, because the $d_\pi-d_\pi$ bonding overlap has a nodal plane between the two Si atoms (see Supporting Information, Figure S-3B).

Bonding Nature and Electronic Structures of the Platinum(I) and Palladium(I) Analogues. Two-electron oxidation of $Pd_2(\mu\text{-}Si_2H_4)(PH_3)_4$ and $Pt_2(\mu\text{-}SiH_2)_2(PH_3)_4$ considerably shortens the Pt−Pt and Pd−Pd distances and considerably lengthens the Si−Si distance, as shown in parts D and F of Figure 1. Consistent with these geometry changes, the occupancy number of the Si−Si bond becomes zero and those of the M−Si σ- and σ*-bonds become 1.683 e and 0.521 e, respectively, by the two-electron oxidation, as shown in Table 1. The similar occupation numbers are calculated in the platinum(I) analogue. The above results indicate that these complexes should be characterized as a typical bis(μ-silylene)-bridged dinuclear complex with a M−M σ-bond, $[M_2(\mu\text{-}SiH_2)_2(PH_3)_4]^{2+}$. Because the palladium(0) complex is characterized as a μ-disilene-bridged dinuclear complex,[9] it is clearly concluded that the interconversion between the bis(μ-silylene)-bridged form and the μ-disilene-bridged one can be achieved by two-electron oxidation/two-electron reduction in the dinuclear palladium complex. In the platinum analogue, on the other hand, the interconversion between the bis(μ-silylene)-bridged form with a weak Si−Si bonding interaction and the bis(μ-silylene)-bridged form with a Pt−Pt σ-bond is achieved by two-electron oxidation/two-electron reduction in the dinuclear platinum complex, as shown in Scheme 5.

The discussion of electronic structure and bonding nature of $[Pt_2(\mu\text{-}SiH_2)_2(PH_3)_4]^{2+}$ and $[Pd_2(\mu\text{-}SiH_2)_2(PH_3)_4]^{2+}$ is omitted here because they are essentially the same as those of $[Rh_2(\mu\text{-}SiH_2)_2(PH_3)_4]$.

The reaction energy by the two-electron oxidation was calculated with various computational methods, as shown in Table 2A. All the methods including the DFT method provide a similar reaction energy. It should be noted that the two-electron oxidation is remarkably endothermic in these Pt and Pd complexes. These results indicate that the interconversion between the two forms cannot be achieved electrochemically. Incorporation of solvent effects with the DPCM method considerably reduces the endothermicity, but it is still very large. However, the two-electron oxidation by Cl_2 is considerably exothermic, as shown in Table 2B, where only the M−Cl distance was optimized without any geometry change of the $[M_2(\mu\text{-}SiH_2)_2(PH_3)_4]$ moiety (see Supporting Information, Figure S-4, for the optimized geometry). The stabilization by the presence of Cl^- results from the electrostatic interaction of Cl^- with $[M_2(\mu\text{-}SiH_2)_2(PH_3)_4]^{2+}$ and the electron donation from Cl^- to the M center; actually, the Cl atomic population decreases by 0.233 e and the Pd atomic population increases by 0.055 e in $[Pd_2(\mu\text{-}SiH_2)_2(PH_3)_4]Cl_2$. The similar electron populations are observed in the Pt analogue (see Supporting Information, Table S-3). Solvent effects calculated with the DPCM method somewhat increase the exothermicity, as shown in Table 2B.

Although the two-electron oxidation of dinuclear platinum(0) complexes has not been reported to our knowledge, one-electron oxidation of a phosphido-bridged dinuclear platinum(0) complex, $Pt_2(\mu\text{-}PR_2)_2(PR_3)_4$, was experimentally carried out with tetracyanoethylene and ferrocene,[33] in which the formation of the Pt−Pt bond by oxidation was reported; strictly speaking, not a Pt−Pt σ-bond but a Pt−Pt half-bond is formed because one electron still remains in the $d_\sigma-d_\sigma$ antibonding orbital after one-electron oxidation. In the other experimental work, the electrochemical two-electron oxidation of the mononuclear platinum(II) complex, $[Pt(tby)(pip_2NCN)]^+$ (tby = terpyridyl, pip_2NCN = 2,6-bis(1-piperidiyl-methyl)phenyl)), was investigated, and it was reported that the Pt−ligand bond was newly formed by the oxidation.[34] Thus, we wish to theoretically propose that the interconversion between the bis(μ-silylene)-bridged form and the μ-disilene-bridged form by oxidation/reduction is not unusual but can be achieved experimentally with appropriate oxidation reagent and solvent.

Significant Differences in Two-Electron Reduction/Two-Electron Oxidation between the Rhodium Complex and the Other Palladium and Platinum Complexes. As shown in Table 3, the two-electron reduction of the dinuclear rhodium(0) complex induces the population changes opposite the changes observed by the two-electron oxidation of the palladium(0) and platinum(0) analogues. Despite the similar population changes, the two-electron reduction of the dinuclear rhodium(0) complex, $Rh_2(\mu\text{-}SiH_2)_2(PH_3)_4$, occurs with moderate endothermicity in the gas phase and with moderate exothermicity in polar solvent such as THF. In this two-electron reduction, the $d_\sigma-d_\sigma$ antibonding orbital accepts two electrons, but these two electrons are not localized on the d orbital of Rh but delocalized over the whole molecule. In particular, the electron population of the Si_2H_4 moiety considerably increases. This indicates that the $d_\pi-\pi$* back-donation interaction becomes strong to stabilize the anion species, $[Rh_2(\mu\text{-}Si_2H_4)(PH_3)_4]^{2-}$. As a result, the two-electron reduction of the dinuclear rhodium(0) complex is easily achieved. Also, the two-electron oxidation of $[Rh_2(\mu\text{-}Si_2H_4)(PH_3)_4]^{2-}$ easily occurs because the Rh atom takes the −1 oxidation state in $[Rh_2(\mu\text{-}Si_2H_4)(PH_3)_4]^{2-}$ in a formal sense.

On the other hand, the two-electron reduction of the palladium(I) and platinum(I) analogues induces substantially large stabilization energy. In the two-electron reduction, the $d_\sigma-d_\sigma$ antibonding orbital accepts two electrons. This antibonding orbital mainly consists of the d orbital and the π orbital of Si_2H_4. Although the orbital picture is similar in these Rh, Pd, and Pt systems, the d orbitals of the Pd(I) and Pt(I) atoms are at a lower energy than that of Rh(0).[31] As a result, the two-electron reduction of palladium(I) and platinum(I) complexes is substantially exothermic; conversely, the two-electron oxidation of the palladium(0) and platinum(0) complexes is substantially endothermic.

Conclusions

The rhodium(0) complex with composition $M_2(SiH_2)_2(PH_3)_4$ is characterized as a bis(μ-silylene)-bridged di-

(33) Leoni, P.; Pasquali, M.; Fortunelli, A.; Germano, G.; Albinati, A. *J. Am. Chem. Soc.* **1998**, *120*, 9564.
(34) Jude, H.; Bauer, J. A.; Connick, W. B. *J. Am. Chem. Soc.* **2003**, *125*, 3446.

nuclear rhodium(0) complex with a Rh−Rh σ-bond, $Rh_2(\mu\text{-}SiH_2)_2(PR_3)_4$. However, this Rh−Rh σ-bond of $Rh_2(SiH_2)_2(PH_3)_4$ is much weaker than that of $Rh_2(SiH_2)_2(PH_3)_4$, which possesses no bridging ligand. The platinum(0) analogue is characterized as a bis(μ-silylene)-bridged dinuclear complex, $Pt_2(\mu\text{-}SiH_2)_2(PR_3)_4$, with a weak Si−Si bonding interaction, although this is different from the Rh analogue because of the absence of the Pt−Pt σ-bond. The palladium(0) analogue is understood to be the μ-disilene-bridged dinuclear complex $Pd_2(\mu\text{-}Si_2H_4)(PR_3)_4$, in which a Si═Si double bond is involved.

$Rh_2(\mu\text{-}SiH_2)_2(PR_3)_4$ changes to the μ-disilene-bridge form, $[Rh_2(\mu\text{-}Si_2H_4)(PR_3)_4]^{2-}$, by two-electron reduction, because the $d_\sigma-d_\sigma$ antibonding orbital becomes doubly occupied by the two-electron reduction. This two-electron reduction easily occurs with moderate endothermicity in the gas phase and moderate exothermicity in polar solvents. On the other hand, the dinuclear palladium(0) and platinum(0) complexes, $Pd_2(\mu\text{-}Si_2H_4)(PH_3)_4$ and $Pt_2(\mu\text{-}SiH_2)_2(PH_3)_4$, are converted to the bis(μ-silylene)-bridged form with an M−M σ-bond, $[M_2(\mu\text{-}SiH_2)_2(PH_3)_4]^{2+}$ (M = Pd or Pt), by two-electron oxidation with a significantly large endothermicity in the gas phase and a moderately smaller endothermicity in polar solvents. However, the oxidation of these complexes by Cl_2 occurs with considerable exothermicity, and its exothermicity increases in polar solvents.

Summarizing the above results, we wish to propose that the interconversion between the bis(μ-silylene)-bridged dinuclear complex and μ-disilene-bridged dinuclear one is electrochemically achieved in the rhodium complex and that the two-electron oxidation of the dinuclear palladium(0) and platinum(0) complexes can be performed with strong oxidant in polar solvents, but the reverse, two-electron oxidation, can be carried out electrochemically.

Acknowledgment. This work was financially supported in part by the Ministry of Education, Culture, Science, Technology, and Sports through Grants-in-Aid on basic research (No. 15350012), Grants-in-Aid on priority areas "Reaction Control of Dynamic Complexes" and "Exploitation of Multi-Element Cyclic Molecules" (No. 412 and 420), Grants-in-Aid on Creative Science Research, and the NAREGI Nanoscience Project. All calculations were carried out on a SGI workstation in the Institute for Molecular Science (Okazaki, Japan) and Pentium IV-cluster systems of our laboratory.

Supporting Information Available: Figures of Hartree−Fock orbitals and Kohn−Sham orbitals near the HOMO and LUMO of $Rh_2(\mu\text{-}SiH_2)_2(PH_3)_4$, contour maps of $d_\pi-d_\pi$ bonding and back-donation from d_π to the unoccupied p orbital of SiH_2 or the π* orbital of Si_2H_4 in $M_2(SiH_2)_2(PH_3)_4$ (M = Pd or Pt), and optimized geometries of $[M_2(\mu\text{-}SiH_2)_2(PR_3)_4]Cl_2$ (M = Pd or Pt). Tables of occupation numbers calculated with the DFT/BS-II method, basis set effects on the energy change by two-electron reduction of $Rh_2(\mu\text{-}SiH_2)_2(PH_3)_4$, and the electron populations of $[Pd_2(\mu\text{-}Si_2H_4)(PH_3)_4]$, $[Pt_2(\mu\text{-}SiH_2)_2(PH_3)_4]$, $[Pd_2(\mu\text{-}SiH_2)_2(PH_3)_4]Cl_2$, and $[Pt_2(\mu\text{-}SiH_2)_2(PH_3)_4]Cl_2$. This material is available free of charge via the Internet at http://pubs.acs.org.

OM040038A